Journal of Proteomics 225 (2020) 103862

Contents lists available at ScienceDirect

Journal of Proteomics

journal homepage: www.elsevier.com/locate/jprot

Comparative analysis of the intracellular responses to disease-related aggregation-prone proteins

Andre Melnik[a,1], Valentina Cappelletti[a,b,1], Federico Vaggi[c], Ilaria Piazza[a,b], Marco Tognetti[a,b], Carmen Schwarz[a], Gea Cereghetti[a], Mennat Allah Ahmed[a], Martin Soste[a], Kent Matlack[f], Natalie de Souza[b], Attila Csikasz-Nagy[d,e], Paola Picotti[a,b,*]

[a] Institute of Biochemistry, Department of Biology, ETH Zurich, CH-8093 Zurich, Switzerland
[b] Institute of Molecular Systems Biology, Department of Biology, ETH Zurich, CH-8093 Zurich, Switzerland
[c] Amazon, Seattle, WA, USA
[d] Randall Division of Cell and Molecular Biophysics, King's College London, SE1 1UL London, United Kingdom
[e] Faculty of Information Technology and Bionics, Pázmány Péter Catholic University, 1083 Budapest, Hungary
[f] Whitehead Institute for Biomedical Research, MIT, 455 Main Street, Cambridge, MA 02142, USA

ARTICLE INFO

Keywords:
Protein aggregation
Yeast
Neurodegenerative diseases
Quantitative proteomics
FUS
TDP43
αSyn
Aβ42
HTT
GFP
Amyloid

ABSTRACT

Aggregation-prone proteins (APPs) have been implicated in numerous human diseases but the underlying mechanisms are incompletely understood. Here we comparatively analysed cellular responses to different APPs. Our study is based on a systematic proteomic and phosphoproteomic analysis of a set of yeast proteotoxicity models expressing different human disease-related APPs, which accumulate intracellular APP inclusions and exhibit impaired growth. Clustering and functional enrichment analyses of quantitative proteome-level data reveal that the cellular response to APP expression, including the chaperone response, is specific to the APP, and largely differs from the response to a more generalized proteotoxic insult such as heat shock. We further observe an intriguing association between the subcellular location of inclusions and the location of the cellular response, and provide a rich dataset for future mechanistic studies. Our data suggest that care should be taken when designing research models to study intracellular aggregation, since the cellular response depends markedly on the specific APP and the location of inclusions. Further, therapeutic approaches aimed at boosting protein quality control in protein aggregation diseases should be tailored to the subcellular location affected by inclusion formation.

Significance: We have examined the global cellular response, in terms of protein abundance and phosphorylation changes, to the expression of five human neurodegeneration-associated, aggregation-prone proteins (APPs) in a set of isogenic yeast models. Our results show that the cellular response to each APP is unique to that protein, is different from the response to thermal stress, and is associated with processes at the subcellular location of APP inclusion formation. These results further our understanding of how cells, in a model organism, respond to expression of APPs implicated in neurodegenerative diseases like Parkinson's, Alzheimer's, and ALS. They have implications for mechanisms of toxicity as well as of protective responses in the cell. The specificity of the response to each APP means that research models of these diseases should be tailored to the APP in question. The subcellular localization of the response suggest that therapeutic interventions should also be targeted within the cell.

1. Introduction

Protein aggregation diseases, including several neurodegenerative diseases, are associated with the accumulation of specific protein aggregates in cells and tissues. The proteinaceous components of the aggregates differ depending on the disease. For example, αSynuclein (αSyn)-containing aggregates (also called Lewy bodies) are typical of Parkinsonism. Proteins with lengthened polyglutamine (polyQ) stretches characterize polyQ disorders; an example is huntingtin (HTT), which is implicated in Huntington's disease. TAR DNA-binding protein

* Corresponding author at: Institute of Biochemistry, Department of Biology, ETH Zurich, CH-8093 Zurich, Switzerland.
E-mail address: picotti@imsb.biol.ethz.ch (P. Picotti).
[1] Equal contribution.

https://doi.org/10.1016/j.jprot.2020.103862
Received 16 January 2020; Received in revised form 29 May 2020; Accepted 2 June 2020
Available online 12 June 2020

(TDP43) and fused in sarcoma (FUS) inclusions are observed in patients with amyotrophic lateral sclerosis. Aggregates of the amyloid-β peptide (Aβ42) and the protein Tau accumulate in brains of patients with Alzheimer's disease. The actual effectors of toxicity can be either the aberrant conformations of the protein, the aggregates or inclusions, the aggregation process itself, or oligomeric intermediates. Different pathogenic mechanisms have been proposed including membrane damage, saturation of quality control systems, co-sequestration of cytoprotective factors, and direct damage of specific functional modules [1–6].

Disease-related aggregation-prone proteins (APPs) differ in primary sequence and three-dimensional structure, but the physico-chemical features of mature aggregates, termed amyloid aggregates, are conserved irrespective of the protein they contain. Amyloids are unbranched fibrillary structures with a repeating unit consisting of β strands that run perpendicular to the fiber axis, forming a cross-β sheet of variable length. In electron micrographs, amyloids appear as long, nonbranched filaments with diameters of 6–12 nm [7]. Amyloids from different proteins share features such as protease resistance, insolubility in detergents, and capability to bind hydrophobic dyes such as thioflavin T and Congo Red.

APPs form inclusions in a variety of cell types and model organisms [8–13]. The appearance of intracellular foci is accompanied by dose- and time-dependent cytotoxicity, and mutations that increase the propensity of the APP to aggregate also increase toxicity [14,15], thus supporting the hypothesis of a toxic gain of function upon aggregation. Genetic screens have identified genes that significantly reduce or enhance cytoxicity of individual APPs [14,16–23]; some of these genes affect the predisposition for the respective human disease [22,23]. Intriguingly, genetic interactors of different APPs show only partial overlap suggesting that different APPs act through different intracellular mechanisms.

Overall, these data raise two questions: 1. Is the cellular response to protein aggregates specific to the protein that aggregates or can a generic response to APP aggregates be identified? 2. When aggregates of a single protein form, is the cellular response similar to when global protein misfolding is induced, for example by thermal stress?

To determine whether there is a generalized response to APPs, we comparatively analysed the responses of cells to different APPs using a well-characterized set of yeast models of APP toxicity. In these models, different APPs are expressed in *Saccharomyces cerevisiae* under control of the same promoter and form intracellular inclusions. As controls for the effects of generalized protein aggregation and of protein overexpression we used cells subjected to thermal shock and cells expressing a protein that does not form aggregates, respectively. To identify pathways that respond to the aggregation process, we performed phenotypic analyses, proteomic and phosphoproteomic measurements. Our data indicate that there is no generalized response to protein aggregation, but that the response depends on the aggregating protein, and suggest that APPs trigger specific compartmentalised responses dependent on the subcellular location of the inclusions.

2. Results

2.1. Phenotypic analysis of cells that express amyloidogenic proteins

To investigate how eukaryotic cells respond to intracellular aggregates of different disease-related APPs, we exploited a set of yeast strains that individually express five APPs involved in human diseases: αSyn, FUS, HTT, TDP43, and Aβ42 (Fig. 1, panel a and supplementary discussion). These proteotoxicity models are directly comparable because the different APPs are expressed under control of the same (galactose-inducible) promoter and in the same genetic background (*S. cerevisiae* W303). Previous studies showed that expression of these APPs results in the formation of intracellular inclusions that are toxic to yeast cells with mechanisms relevant to human disease [19][14,17,20,24–31] (and supplementary discussion). As a control, we used a yeast strain transformed with an empty vector (EV). To evaluate the generic responses of yeast to protein overexpression, we used a yeast strain that expresses the green fluorescent protein (GFP) under control of the same promoter used to express the APPs. Further, we compared the responses of yeast strains to aggregates of specific APPs to those of yeast cells undergoing generalized protein aggregation induced by heat shock, a condition known to trigger intracellular aggregation of various proteins and induction of protein quality control systems [32,33].

To confirm that expression of the five human APPs resulted in cellular toxicity in yeast, we measured the growth of the yeast expressing each of the APPs and the controls and performed spot assays on inductive (galactose containing) and non-inductive (glucose-containing) solid media. Growth was severely impaired by the expression of all the APPs relative to the control and the GFP-expressing strains (Fig. 1, panel c). The most pronounced effect was observed for the αSyn-expressing strain, for which a substantial reduction in biomass concentration was also observed relative to the control (Fig. 1, panel d). We confirmed the formation of intracellular inclusions by fluorescence microscopy using GFP-tagged αSyn, TDP43, and HTT and YFP-tagged FUS. In each case, we detected the formation of multiple GFP- or YFP-positive cytoplasmic inclusions between 30 min and 1 h after induction of expression (Fig. 1, panel b). In the strain expressing GFP alone, a homogeneous cytoplasmic distribution of the fluorescent signal was observed. Formation of intracellular inclusions by Aβ42 was previously shown to be inhibited when the peptide was fused with GFP. Therefore, formation of Aβ42 intracellular inclusions was confirmed by immunofluorescence as previously reported [24]. Aβ42 inclusions were localized in both the cytosol and the endoplasmic reticulum (ER) (Fig. 1, panel b). These data demonstrate that, in our models, expression of the different APPs results in the formation of intracellular inclusions and is toxic to yeast cells. The extent of toxicity depends on the expressed APP. Expression of GFP alone is not toxic to yeast.

2.2. APP aggregation results in widespread alterations in protein abundance and phosphorylation

To investigate the responses of cells to the formation of intracellular inclusions of different APPs, we analysed the proteomes and phosphoproteomes of the APP-expressing and control strains using mass spectrometry-based label-free shotgun proteomics. Protein abundance changes are influenced by transcriptional and translational responses and protein degradation events. Monitoring changes in the phosphoproteome provides an additional layer of information regarding regulatory and signalling events [34].

First, we profiled proteome changes in yeast cells expressing the different APPs relative to cells expressing the EV at 6, 12, 18, and 24 h after induction of expression. We obtained relative abundance measurements for 4345 proteins (Table 1). The number of significantly down-regulated proteins (q-value cutoff: 0.05, fold-change cutoff: −2) ranged from 166 for the GFP-expressing strain to 1073 for the FUS-expressing cells. The number of significantly up-regulated proteins (q-value cutoff: 0.05, fold-change cutoff: 2) ranged from 83 for the GFP-expressing strain to 395 for the cells that expressed αSyn (Table 2). The fraction of proteins that changed abundance (out of all detected proteins) increased over time in cells expressing each of the APPs (Fig. 2, panel a), from 4.9% at 6 h to 20.6% at 24 h for the Aβ42 model, from 1.5% at 6 h to 15.3% at 24 h for the TDP43 model, from 4.7% at 6 h to 32.5% at 24 h for the FUS model and from 0.3% at 6 h to 8.8% at 24 h for the GFP-expressing strain (Fig. 2, panel a). In both the αSyn and HTT models, only a small fraction of the proteome had changed abundance at 6 h (0.7% and 0.5%, respectively); however, after 12 h 12.7% and 6.2% of the measured proteins differed in abundance from the pre-induction time point, and these numbers remained approximately constant at 18 and 24 h (Fig. 2, panel a). Interestingly, the fraction of down-regulated proteins was higher than the fraction of up-

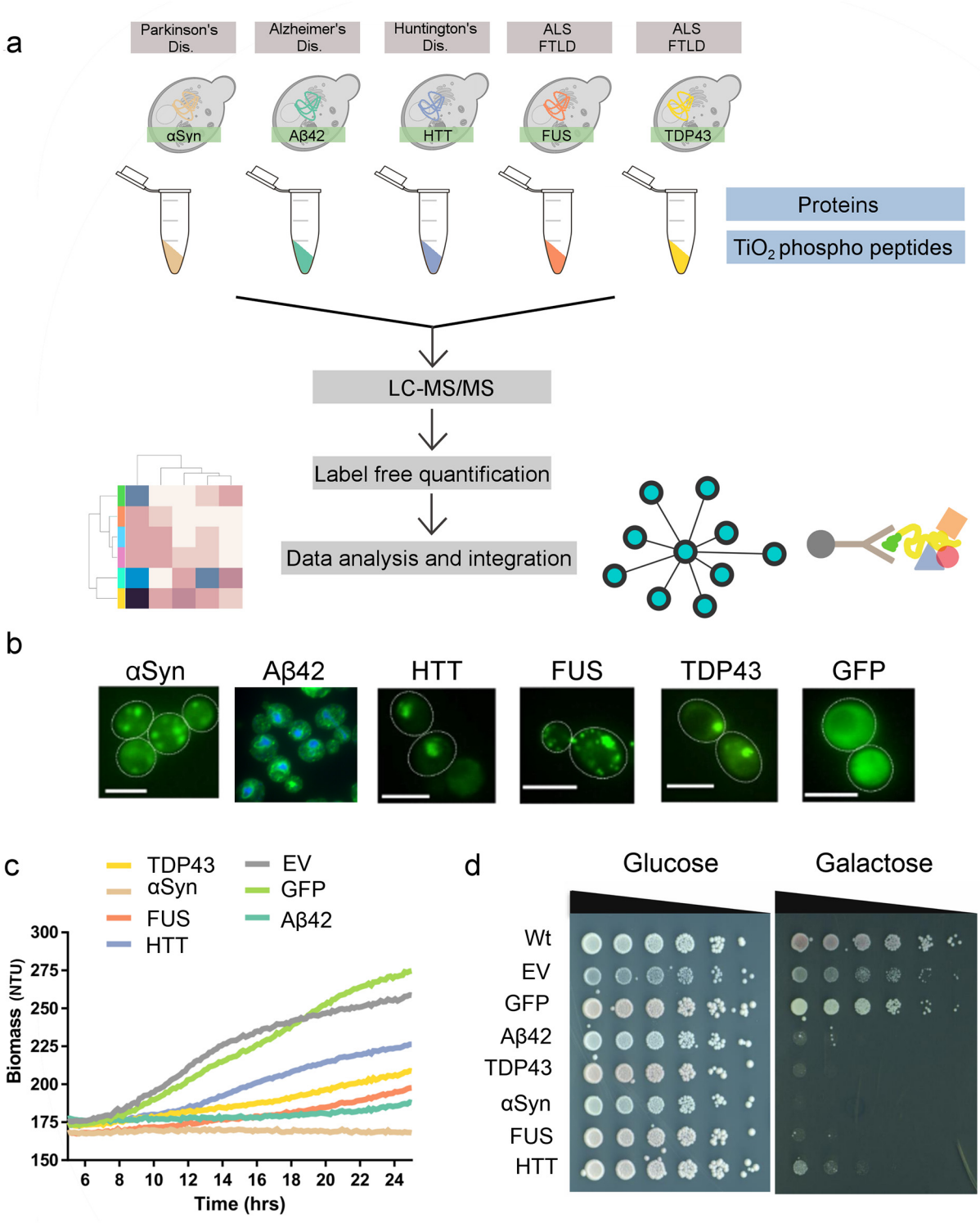

Fig. 1. Yeast models of proteotoxicity to analyse the cellular response to aggregation prone proteins (APPs). (a) The schematic shows our experimental design. We perform quantitative proteomics and phosphoproteomics on yeast strains expressing one of the five indicated APPs and use functional enrichment analysis to identify altered biological processes. (b) Representative fluorescence micrographs of the indicated yeast strains 1 h after induction of APP expression. In all APP-expressing strains other than the Aβ42 strain, the micrograph shows GFP fused to the APP. In the Aβ42 strain, the micrograph shows immunofluorescence staining of Aβ42. The control panel (GFP) shows fluorescence of GFP alone. Scale bars represent 10 μm. (c) Growth curves of the indicated yeast strains over time, after induction of the APP. Biomass is measured via scattered light upon excitation at 620 nm. NTU, nephelometric turbidity unit. EV, empty vector. (d) Growth on solid media of the indicated yeast strains under decreasing concentrations of galactose (inducer) and glucose (non-inducer).

regulated proteins in most cases, with 26% of the total number of identified proteins down-regulated in the FUS-expressing strain. The exception was the αSyn model in which the number of up-regulated proteins exceeded the number of down-regulated proteins by approximately 50% (Fig. 2, panel a).

Next, we analysed the phosphoproteomes at 6 h after induction of expression of the APPs. We identified a total of 3137 phosphosites across all conditions mapping to 1157 proteins (Table 3 and

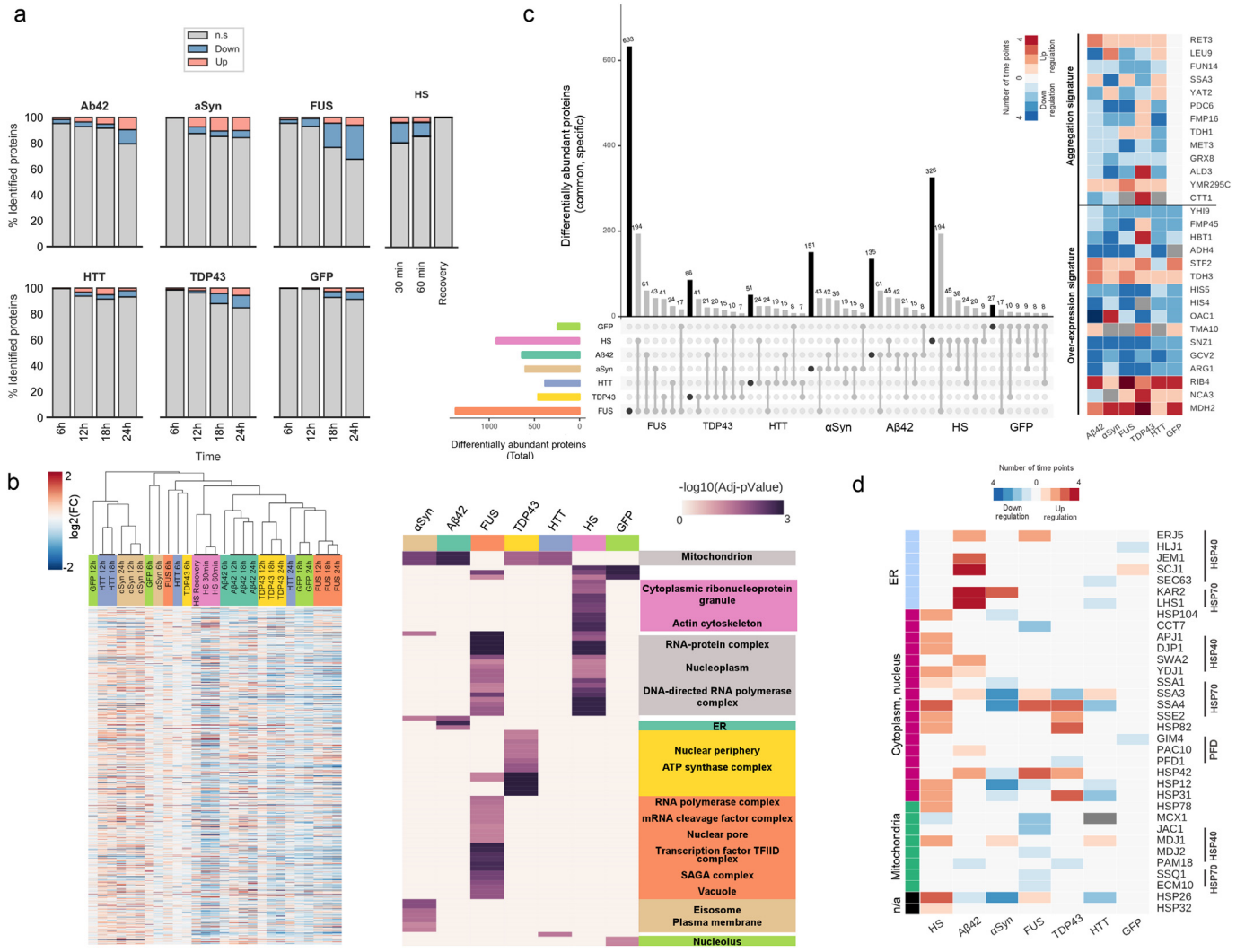

Fig. 2. The cellular response to APP expression is largely specific to the aggregating protein. (a) The fraction of proteins that change abundance in the yeast strains at the indicated times after induction. HS indicates wild type yeast subject to heat shock at 42 °C for 30 or 60 min, with or without a 2 h recovery period at 30 °C. For APP and GFP strains, we measured abundance relative to the EV-containing yeast. For the HS experiment, we measured abundance relative to yeast grown at 30 °C. (b) The heat map (left) shows hierarchical clustering of protein abundance changes across time points and conditions. Coloured scale bar represents relative protein abundances. The right panel shows functional categories enriched for changing proteins in the indicated strains. Cellular component classes are shown. The significance level of a category is indicated by the adjusted *p*-value, the range of which is reported in the colour scale bar. (c) Pairwise comparison of proteins that change abundance between the indicated strains; the number of changing proteins is shown for each comparison. The bar plot (left) shows the total number of changing proteins for each strain relative to control. Heat maps (right) show proteins that change in all APP strains (aggregation signature) and in all experimental strains (overexpression signature). (d) Protein abundance changes of chaperones in the indicated APP strains and in wild type yeast after heat shock, clustered according to cellular locations.

Supplementary Figure 1). In agreement with results at the protein level, the sample showing the highest number of differentially regulated phosphosites (q-value cutoff: 0.05, fold change cutoff: 2) was the FUS-expressing strain (1498 phosphosites). Significantly fewer regulated phosphosites were detected in cells expressing the other APPs: 19 for Aβ42, 277 for αSyn, 36 for HTT, and two for TDP43. We detected no differentially regulated phosphosites in the GFP-expressing control strain. The temporal trend of protein abundance variations indicates a progressive alteration of cell homeostasis as a consequence of the expression of the different APPs. Notably, the expression of GFP also significantly affected the expression of a small fraction of the proteome (4%), suggesting that this perturbation is not neutral.

2.3. Proteome responses are APP specific

We analysed the specificity of cellular responses to expression of different APPs and the similarity to responses of cells undergoing generalized protein aggregation. As a model for global and nonspecific protein aggregation, we analysed yeast cells subjected to heat shock. Heat-shock was previously shown to result in formation of intracellular protein aggregates involving a large fraction of the proteome [35]. We incubated wild-type yeast cells for 30 and 60 min at 42 °C, followed by a recovery phase of 2 h at 30 °C. We performed quantitative proteomics and phosphoproteomics analyses and quantified a total of 3042 proteins across the different conditions (Table 2), relative to cells grown at 30 °C. In cells heat shocked for 30 min, 27.8% of the proteome changed abundance compared to the control; 667 proteins were down-regulated and 177 up-regulated. After 1 h, levels of 20.7% of the measured proteins were altered; levels of 465 proteins were decreased, and levels of 164 proteins were increased. After the recovery phase, only 0.3% of the proteome varied in abundance, reflecting restoration of protein homeostasis upon return to the optimal growth temperature (Fig. 2, panel a).

We then compared the responses of heat-stressed cells to cells expressing individual APPs. Hierarchical clustering of protein abundance

changes across all the conditions and time points revealed the presence of condition-specific signatures (Fig. 2, panel b). The three samples from the heat shock treatment (30 min, 1 h, and after recovery) formed a distinct cluster (Fig. 2, panel b - cluster cutoff 0.5) mainly characterized by down-regulated proteins. This possibly reflects the reduction in protein synthesis and increase in protein degradation that characterizes the heat-shock response [36,37]. A second cluster included the αSyn (12, 18, and 24 h) and HTT (12 and 18 h) models. For both Aβ42 and the FUS models we observed separate clusters, each including almost all the time points. Only the 18-h and 24-h time points for the GFP and HTT models were joined into clusters, indicating the activation of specific signatures of protein expression in the late stages of the responses to these proteins. A heterogeneous cluster included the 6 h and 12 h time points for most models, likely as a result of the small number of differentially abundant proteins detected at these time points. Application of t-SNE dimensionality reduction to capture clustering patterns confirmed the existence of strain-specific responses (Supplementary Figure 2). Similarly, we detected no common phosphorylation patterns, and differential phosphorylation events showed minimal overlap (Supplementary Figure 1).

To evaluate whether any common response could be identified between pairs of differently stimulated yeast strains, we performed a pairwise comparison of proteome (Fig. 2, panel c) and phosphoproteome signatures (Fig. S2) across the different models. At the protein level we detected little intersection among sets of regulated proteins from the different APP-expressing cells. The GFP model consistently showed the lowest number of common deregulated proteins compared to strains expressing APPs (Fig. 2, panel c). Only a small set of proteins changed their abundance in response to all APPs but not GFP; we term this the “aggregation signature” (Fig. 2, panel c). Among proteins from this group, we detected an overall up-regulation of Ret3p, which mediates the retrograde transport from the ER to the Golgi apparatus, and Ymr295cp, a protein of unknown function. The remaining 11 proteins showed divergent expression profiles in the five APP models. Notably, Ssa3p, which regulates protein folding and aggregation, was up-regulated in Aβ42, FUS, and HTT models but down-regulated in the TDP43- and αSyn-expressing strains. The Ctt1p cytosolic catalase was affected in all the models at multiple time points, suggesting a role of the oxidative stress response in APP-mediated toxicity. We detected 16 proteins that significantly changed in abundance in at least one time point upon expression of all exogenous proteins including GFP. We term this set the “overexpression signature” (Fig. 2, panel c). Within this set, several proteins from amino acid metabolism pathways (His4p, His5p, Arg1p, Gcv2p) showed a consistent down-regulation, whereas gluconeogenic enzymes Tdh3p and Mdh2 were consistently up-regulated.

We next focused on molecular chaperones, a class of proteins known to be induced in response to protein aggregation. In cells subjected to heat shock, we detected a pronounced up-regulation of various chaperone proteins (as defined by Gong et al. [38]) from different cellular locations (Fig. 2, panel d), in line with previous reports and with the known roles of these proteins in the response to proteotoxicity [32,33]. Eleven out of 15 chaperone proteins changed abundance in the heat-shocked strains and in one or multiple APP models, revealing the activation of chaperone-mediated pathways in all cases of exogenous expression. Interestingly, APP-specific chaperone patterns were detected (Fig. 2, panel d). In the Aβ42 model, we observed induction of ER-resident Hsp70 and Hsp40 chaperones, known to be involved in the translocation and folding of proteins in the ER and in the ER-associated degradation pathway (Fig. 3); this may reflect the fact that the Aβ42 is fused to an ER-targeting sequence in this model [24]. Expression of αSyn resulted in the depletion of various cytosolic chaperones relative to the control and in a slight induction of a mitochondrial and of an ER-associated chaperone. In the FUS and TDP43 models we observed an induction of a specific set of cytosolic chaperones and the depletion of specific mitochondrial and other chaperones. Expression of HTT induced complex chaperone alterations involving induction and depletion events. These results indicate that inclusion formation by the different APPs results in APP-specific cellular responses, including chaperone responses.

2.4. APPs induce regulation of different biological processes

To gain insights into pathways and biological processes activated by expression of the different APPs, we performed a functional enrichment analysis on the set of proteins significantly changed in abundance or phosphorylation status in the different proteotoxicity models. Amino acid metabolic pathways were found enriched in all APP-expressing strains and the GFP-expressing strain (Table 4).

The cellular response to αSyn expression involved mitochondrial respiration, ER homeostasis, and eisosome complexes at the plasma membrane (Fig. 2, panel b and Table 4). The expression of the RNA/DNA-binding protein FUS led to alterations in gene expression regulation, chromatin organization, and RNA processing and transport. mRNA-binding proteins were also significantly enriched upon FUS expression Similarly, in the TDP43 model we identified an enrichment in proteins from the biosynthesis pathways of RNA binding proteins (Fig. 2, panel b and Table 4). Proteins from the mitochondrial protein biosynthesis process were enriched in both FUS and TDP43 expressing strains. Functional categories overrepresented in the HTT model were the DNA repair category and several processes associated with synthesis of nucleotides.

In the Aβ42-expressing strain we detected an enrichment in proteins involved in the unfolded protein response, including several chaperones known to localize to the ER (Lhs1p, Kar2p, Scj1p), and ER-associated proteins involved in disulfide bond formation (Mpd1p, Pdi1p, Ero1p, Eug1p), glycosylation (Pmt1p, Ktr1p, and Mcd4), and translocation (Sil1p and Sec72p) (Fig. 3 and Table 2). Proteins involved in ER-associated degradation, ER-to-Golgi trafficking (Erp1/2p, Erv46p, Bos1p), and lipid/inositol metabolism (Dfr1p, Acb1p, Rib1p, Scs3p) were also significantly enriched in the Aβ42 strain compared to the control (Table 2), suggesting an overall involvement of the ER in the response to aggregation of Aβ42 in the context of this yeast model in which Aβ42 is directly fused to an ER-targeting sequence [24]. In the Aβ42-expressing strain, we also detected enrichment in proteins from the reactive oxygen species metabolic process, the pentose-phosphate shunt, glyceraldehyde-3-phosphate metabolic processes and NADP metabolic process, indicating alterations in central carbon metabolism.

Next, we predicted the set of kinases involved in the responses to different APPs. We inferred kinase–substrate interactions from the phosphorylation dataset, integrating consensus motif analysis and context modelling using the NetworKIN algorithm [39]. Few phosphosites were affected in more than one condition (Fig. 4, orange and red nodes). In contrast, we identified several kinases as involved in multiple APP models (Fig. 4, gray nodes). Among these were Cka1 (for which we found an enrichment based on several sites in FUS-, Aβ42-, αSyn-, and HTT-expressing cells), Pkc1 (enriched in strains expressing FUS, Aβ42, and αSyn), and Pho85 (enriched in strains expressing FUS, HTT, and Aβ42) (Table 5).

Taken together, these results indicate that yeast cells have complex responses to the different APPs. Only a few cellular processes, mainly involving metabolic functions, were activated in common, in the different APP expression models. Phosphoproteomic investigation confirmed the existence of APP-specific cellular responses but kinase enrichment analysis also revealed some common regulatory mechanisms activated upon over-expression of different amyloidogenic proteins.

2.5. APPs primarily affect the subcellular location where inclusions form

In our functional enrichment analyses, we noticed that expression of the different APPs affected biological processes connected to the subcellular locations where inclusion formation occurs. αSyn forms inclusions that are initially located at the plasma membrane and that

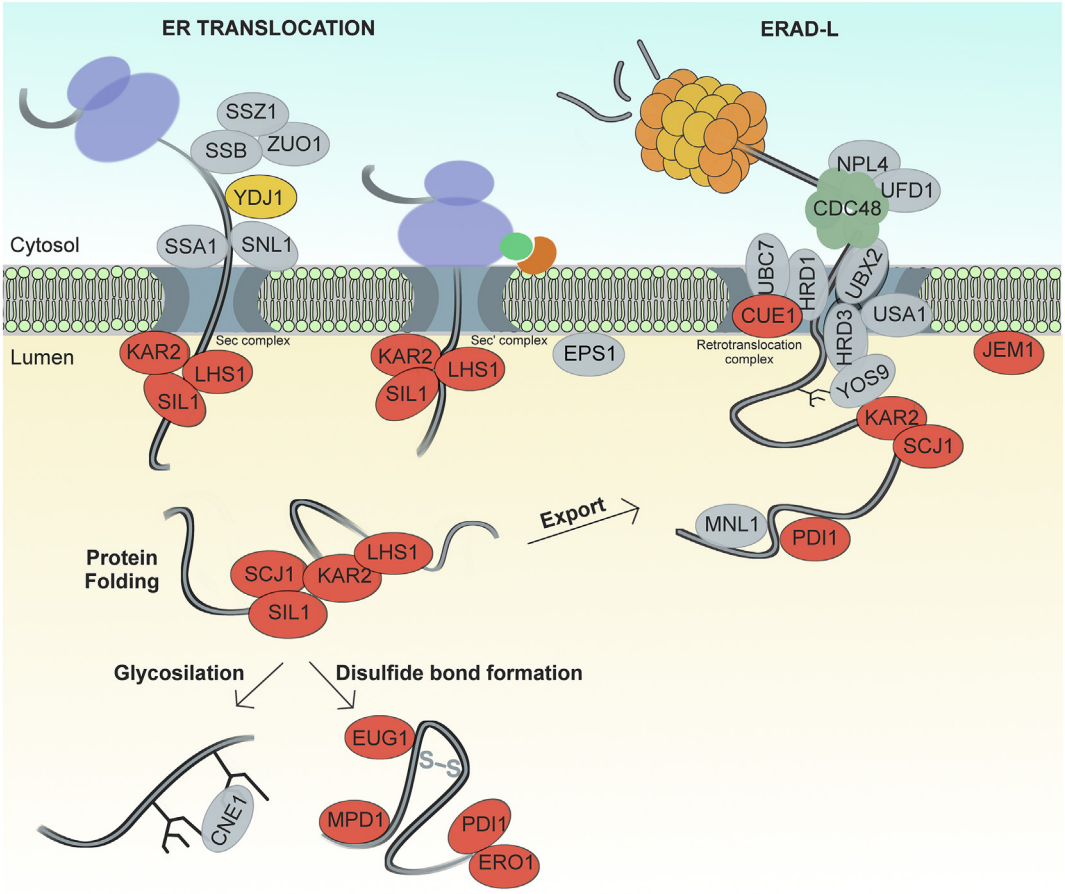

Fig. 3. Protein abundance variations in the protein folding and secretion pathway in the Aβ42 model. Key proteins of the ER secretion pathway are shown. Red nodes represent upregulated proteins while gray nodes represent proteins not changing abundance in the Aβ42 model compared to the control. (For interpretation of the references to colour in this figure legend, the reader is referred to the web version of this article.)

subsequently move to the cytoplasm. In keeping with this, we observe enrichment of eisosome complexes among proteins that change in yeast expressing αSyn; these plasma membrane complexes are known to act as sensors of membrane stress [40] and our observations are therefore consistent with perturbation of the plasma membrane in these strains. Similarly, the Aβ42 peptide forms inclusions in the ER, and we observe an enrichment of ER-specific responses in this model. TDP43 and FUS inclusions co-localize with cytoplasmic ribonucleoprotein bodies, reflected by our observation of altered RNA processing and transport processes and enrichment of mRNA-binding proteins in the response to TDP43 and FUS expression. The one exception to this pattern was the HTT model; HTT inclusions are cytoplasmically located, but we did not observe the activation of specific cytosolic pathways in our enrichment analysis. These observations suggest that the response to the aggregation of the different APPs is driven by the subcellular location where inclusions form.

Indeed, when we extended the GO enrichment analysis to the cellular component term, we observed similar associations. In this analysis, we converted the resulting list of enriched categories to a Boolean matrix of 175 elements and clustered them to detect common regulation patterns (Fig. 2, panel b). Again, we detected strain-specific patterns of enrichment. In addition, enriched cellular components for a particular strain again tended to match the subcellular location of inclusions in that strain. The ER was exclusively enriched in Aβ42-expressing yeast. In the αSyn model, we found a specific enrichment in proteins from mitochondria, plasma membrane, and eisosomes. We observed an enrichment of nuclear proteins (where aggregation of FUS and TDP43 initially takes place [30,41]) in TDP43- and FUS-expressing cells (Fig. 2, panel b), with proteins involved in proton transport connected to ATP synthesis additionally enriched in the TDP43 model. Proteins associated with the acetyltransferase SAGA, transcription factor TFIID, and RNA polymerase complexes were enriched in the FUS model (Fig. 2, panel b), recapitulating the physiological role of the protein in RNA metabolism and transcription regulation. In the HTT model we only observed an enrichment in mitochondria-associated proteins, which was common to most strains. GFP expression resulted only in enrichment in nucleolar proteins.

These data suggest the hypothesis that the cellular responses to the different APPs involve interactions with molecular players at the location of the inclusions. To evaluate this, we sought to identify interaction partners of three different APPs. Using an antibody against the GFP tag, we immunoprecipitated GFP-αSyn, GFP-HTT, and GFP-TDP43 and analysed immunoprecipitates by mass spectrometry after three and six hours of induction of APP expression. The GFP strain was used as control to identify nonspecific interactions (see Material and Methods for details). We identified nine, 61, and 85 interactors for αSyn, HTT, and TDP43, respectively (Table 6) with most proteins detected at both time points. Several proteins involved in RNA processing were found associated to TDP43, supporting our hypothesis. In the αSyn immunoprecipitate, we did not identify any proteins known to localize to the plasma membrane, possibly due to the removal of membrane debris from the cell lysate during protein extraction. Cytosolic chaperone proteins, as well as several proteins involved in protein targeting and export and cytoskeleton organization, were associated with HTT. Several chaperones were identified in the APP immunoprecipitates; Ssc1p, Ssa3/4p, Kar2p, Hsp82p, and Hsp104p associated with at least two APPs. In contrast, Sse1p and Sse2p were uniquely associated with αSyn; Hsc82p, Ydj1p, Pdi1p, Cct8p, and Mdj1p associated only with

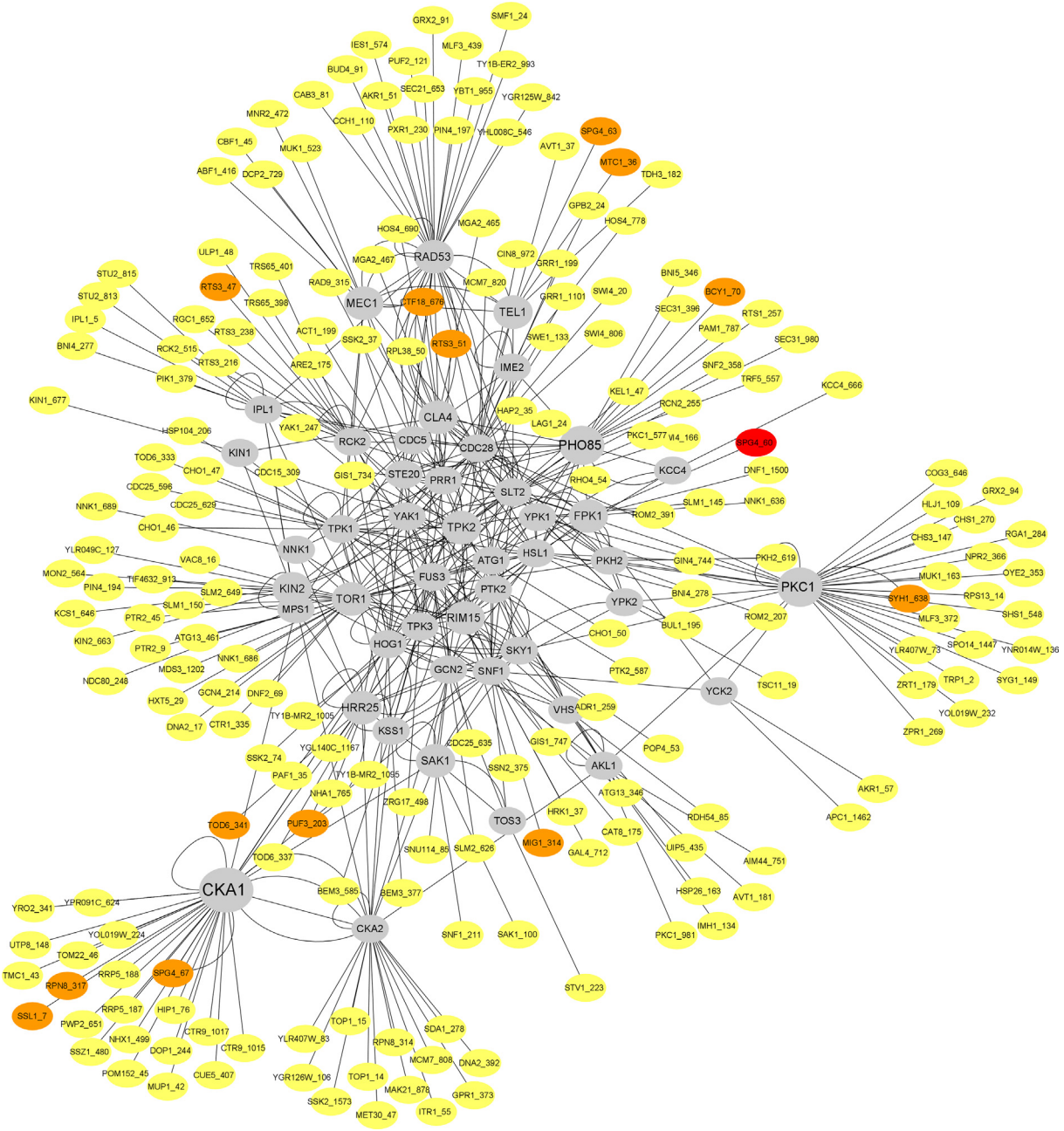

Fig. 4. Changes in phosphorylation in response to APP expression. The coloured nodes in the network show changing phosphosites for all strains. Yellow nodes indicate phosphorylation sites that change in a single strain, orange and red nodes show sites changing in more than one strain, as reported in the legend. Gray nodes show the kinases predicted to be involved in the detected phosphorylation events. Size of the gray nodes is proportional to the number of APP strains in which the kinase was predicted, as reported in the legend. Edges represent protein-protein and genetic interactions between proteins bearing the p-sites and/or the predicted kinase. (For interpretation of the references to colour in this figure legend, the reader is referred to the web version of this article.)

TDP43; and Hsp60p immunoprecipitated only with HTT (Fig. 5, panel a). These data support the existence of APP-specific chaperone responses; whether location-specific physical interactions drive the response to APP expression will need further confirmation.

2.6. Protective and toxic events in yeast expressing APPs

Proteome changes detected in our screen in response to the different APPs may reflect the activation of protective cellular responses or biological processes involved in toxicity of the APP. To differentiate between protective and toxic proteome responses we used information from previous genome-wide genetic screens conducted in the same APP yeast models. These screens identified sets of genes that suppressed or enhanced the toxicity of the respective APP and could play a role in the respective protein aggregation disease [19], [24,42–45]. We reasoned that toxicity suppressors up-regulated or toxicity enhancers down-regulated in our proteomic screens may be involved in processes counteracting the proteotoxic insult. Similarly, the downregulation of suppressors and the upregulation of enhancers may be involved in mechanisms that result in toxicity and ultimately death of yeast cells.

A total of 47 known genetic modifiers of the APPs were found to be differentially abundant in our proteomic analysis. We classified as protective those proteins that were up-regulated in our proteomics analysis that inhibited APP toxicity when the gene was ablated in the previous genetic screen, or that were down-regulated in our analysis and enhanced APP toxicity in the genetic screen. Similarly, we defined

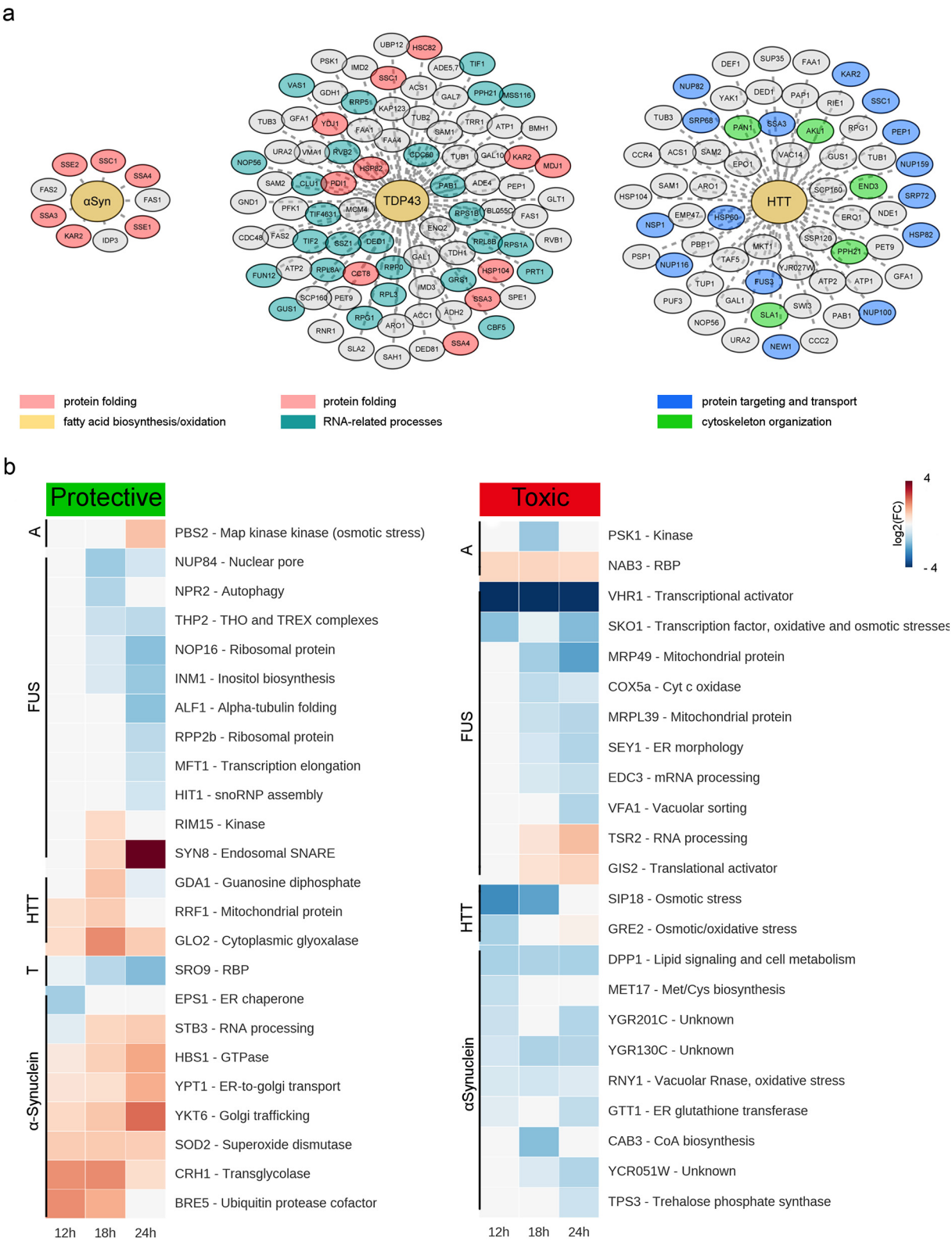

Fig. 5. Genetic and physical interactions with APPs. (a) The networks depict physical interactors of the indicated APPs, colour coded according to their GO annotation. (b) The heat maps show abundance changes over time for proteins previously annotated as genetic interactors of the indicated APP. Proteins are classified as protective or toxic depending on the direction of the abundance change and the nature of the genetic interaction.

as toxic those proteins that were significantly down-regulated in our proteomics dataset and previously annotated as enhancers or that were up-regulated and shown to be suppressors in the genetic screen. In total, we defined 24 proteins as protective. We observed changes in abundances of each of these proteins after 12 h of expression of the APP (Fig. 5, panel b). Among protective proteins for the αSyn model are proteins involved in ER-to-Golgi trafficking (Bre5p, Ykt6p, Ypt1p), response to oxidative stress (Sod2p), and RNA processing (Stb3p and

Hbs1p), and the ER chaperones Eps1. In the FUS model, the protective kinase Rim15 was associated with the phosphorylation of Adr1p and Ssn2p; the latter factors are involved in the regulation of transcription. The proteins protective in the αSyn model were all upregulated upon αSyn expression. The kinase Pbs2p of the HOG signalling pathway is the only protein we classified as protective in the Aβ42 strain; it was upregulated upon Aβ42 expression. We classified the down-regulation of the RNA-binding protein Sro9p, from early to late time points, as protective for cells expressing TDP43. Finally, the up-regulation of Glo2p, Rrf1p, and Gda1p was protective for HTT-expressing cells. In total, we categorized 23 proteins as toxic. These are mainly associated with mitochondria or RNA-related processes in the FUS model, with osmotic stress in the HTT model, and with lipid signalling and cell metabolism in the αSyn model.

3. Discussion

Protein folding is crucially important to life. When globular proteins fail to adopt a functional fold they can assemble into aberrant aggregates, which accumulate intracellularly and have been linked to cellular dysfunction. Protein conformational disease, however, also involves proteins that do not adopt a stable globular fold. In particular, intrinsically disordered proteins/regions (IDP/IDR) are over-represented among disease-associated proteins, with disorder being linked both to normal function as well as to aberrant function in disease; this has led to the proposal of the 'disorder in disorders' (D^2) concept of human disease [46]. All of the proteins in our study fall into this category: they are either IDPs (αSyn and Aβ42), or hybrid proteins including IDRs (FUS, HTT, and TDP43). Many IDPs form aggregates of amyloid nature, which have been associated with human neurodegenerative disorders such as Parkinson's or Alzheimer's disease. The amyloid fold is highly conserved in terms of structure and physico-chemical properties, irrespective of the sequence of the protein involved. Neurodegenerative diseases involving aggregates from different proteins are however characterized by drastically different clinical phenotypes and progression patterns. This may be because aggregates affect different cell types or brain regions in different diseases, as has been shown for some of these pathologies. It is also possible that aggregates of different APPs elicit different cellular responses. Although many studies have addressed the molecular mechanisms underlying APP-induced cytotoxicity, there has been no systematic, global comparison of the cellular responses to different disease-related APPs. Further, it is unclear whether cellular responses to aggregates of a single protein resemble responses of cells to generalized intracellular protein aggregation, as induced for example by an increase in temperature.

Taking advantage of a consistent set of well-characterized yeast proteotoxicity models, we dissected cellular responses to the overexpression of five human APPs and to generalized protein aggregation induced by heat shock. We confirmed prior observations that expression of APPs causes intracellular inclusions and time-dependent toxicity, although different APPs impaired cell growth to different extents. Proteomic and phosphoproteomic analyses revealed a progressive alteration in cellular homeostasis, via APP-specific responses that were markedly different from the response to generalized temperature-induced protein aggregation. Gene ontology enrichment analysis of altered proteins and phosphorylation sites revealed substantial heterogeneity in the processes affected by the different APPs.

Interestingly, specific cellular responses to APPs largely involved the subcellular compartment where inclusions of the APP accumulate. The plasma membrane and membrane-associated eisosome complexes were solely altered in the αSyn model, possibly reflecting a perturbation of membrane architecture upon formation of early aSyn inclusions [47]. Indeed, in the yeast model, α-Syn first localizes to the plasma membrane or the cortical ER, which in yeast underlies the plasma membrane α-Syn has also been reported to associate with lipid rafts and caveolae, eukaryotic lipid domains that share similarities to *eisosomes in yeast and have been proposed to be analogous structures* [48]. Through its N-terminal lipid binding domain, α -Syn is thought to bind to a variety of cellular membranes, including the plasma and mitochondrial membranes [49]. *Indeed*, overexpression of α-Syn also affected mitochondrial respiration and ER homeostasis in our screen, consistent with observations in mammalian models [50,51]. A direct interaction of αSynuclein with mitochondria has been extensively reported [52–54] and linked to disease progression [55].

In the FUS and TDP43 models we detected changes mainly in processes connected to nuclear and RNA binding proteins, transcriptional machineries, chromatin organization, RNA processing and transport. Consistently, FUS and TDP43 are well-established DNA- and RNA-binding proteins implicated in transcriptional regulation and RNA splicing [56]. Despite their default nuclear localization, the two proteins shuttle to the cytosol under stress or pathological conditions, where they can bind stress granules and form inclusions [19,28]. The enrichment that we see for RNA processing and mRNA-binding proteins, as well as the cytoplasmic localization of FUS and TDP43 inclusions, could reflect this association with stress granules. Indeed, the 66% of all RBPs we identified as enriched in the FUS model, half of which have human orthologues, have been previously shown to localize to stress granules or p-bodies under stress conditions [57]. We were also able to detect a physical interaction of TDP43 with several yeast RNA-binding proteins. Finally, the mitochondrial protein biosynthesis process was also enriched in both FUS and TDP43 models, mirroring the severe mitochondrial dysfunction in ALS pathogenesis [58].

In the Aβ42 model, we found an enrichment of ER-associated chaperones, genes involved in the unfolded protein responses, ER-associated degradation, and ER-to-Golgi trafficking. Again, the involvement of ER-associated processes in response to expression of Aβ42 is consistent with our observation across models that the cellular response to APP expression takes place at least in part at the location at which it accumulates. In this case, the response likely reflects targeting of Aβ42 to the ER via fusion to a signal sequence and the formation of ER-associated Aβ42 oligomers in the yeast model [24]. We note that, physiologically, Aβ42 is not directly targeted to the ER. The 30-fold increase in expression of the transcription factor Hac1, together with the enrichment in UPR-regulated genes, supports activation of the unfolded protein response (UPR) likely to restore ER homeostasis after the perturbation induced by Aβ42 aggregation [59–61]. In addition, we identified an enrichment in the oxidative stress response as well as in the glycolysis and pentose shunt pathways, paralleling alterations in brain metabolism seen in Alzheimer's disease patients [26,62,63]. Induction of an oxidative stress response by overexpression of Aβ42 is further supported by the up-regulation, from early to late time points, of the cytoplasmic antioxidant protein Tsa1, known to protect yeast from the oxidative stress caused by misfolded or aggregated proteins. Lastly, in the HTT model the enrichment we see for DNA repair and synthesis of nucleotides processes could indicate DNA fragmentation, previously associated with HTT toxicity together with the loss of nuclear envelope integrity [64].

The response of chaperone proteins to expression of the different APPs also supports the notion that there is a link between subcellular location of inclusions and that of the response. Chaperones clearly responded to APP expression in all aggregation models, but the response was qualitatively and quantitatively different, depending on the expressed APP. We often observed changes for compartment-specific chaperones associated with APPs that formed inclusions at the corresponding subcellular location. For example, mainly ER-specific chaperones were up-regulated in the Aβ42 model, reflecting the ER localization of Aβ42 inclusions [24], while the TDP43 model, where inclusions are formed in the cytosol, showed upregulation of mainly cytosolic chaperones. In the heat-shocked sample as well, mainly cytosolic promiscuous chaperones were up-regulated, some of which also responded to the overexpression of specific APPs.

Overall, our data suggest that cells specifically respond to the

overexpression of the different APPs by activating biological pathways associated with the subcellular compartment where protein inclusions accumulate. Such responses could be triggered by local damages at the aggregation site, sequestration of compartment-specific factors into the aggregates or saturation of compartment-specific quality control systems. This in turn emphasizes the need to tailor therapeutic manipulations aimed at boosting protein quality control to the subcellular compartment affected by the aggregation process [65]. In addition, care should be taken when designing research models to study intracellular aggregation, since the cellular response depends markedly on the specific APP and the location of inclusions.

Common responses to different APPs mostly included functionally unrelated proteins and proteins involved in the oxidative stress response and ER-to-Golgi trafficking, while the general response to overexpression mostly involved proteins involved in amino acid metabolic pathways, possibly as a consequence of the energetic burden that the production of a heterologous protein entails. In most models, the fraction of downregulated proteins was higher than that of upregulated proteins in response to APP expression, which we also observed in the response to heat shock. This may indicate the activation of protein degradation systems, such as autophagy, in response to protein aggregation, or the trapping and precipitation of proteins in APP aggregates.

Proteins that responded to the expression of different APPs should reflect both toxicity pathways and protective responses that counteract the proteotoxic insult. To discriminate between these two scenarios, we cross-referenced our proteomics dataset with recently published lists of genetic modifiers of APP toxicity and report putative components of toxicity mechanisms or protective regulatory programs, which may be followed up in future studies.

In conclusion, our systematic proteomic and phosphoproteomic study provides global insight into the cellular effects of human disease-associated APPs in yeast. Further work will be needed to determine if the APP-specific responses we observe in these models, as well as the intriguing link between location of inclusions and of cellular response, also apply to human cells.

Supplementary data to this article can be found online at https://doi.org/10.1016/j.jprot.2020.103862.

Author contributions

P.P. conceived and supervised the project and wrote the manuscript. A.M. designed and performed experiments, analysed the data, and wrote parts of the manuscript. V.C. designed and performed experiments, analysed the data, and wrote the manuscript. F.V. analysed the data. A.C.N. supervised part of the project. I.P. designed and performed immunoprecipitation experiments. CS, GC, MT, MS and MAA performed experiments and analysed data. KM prepared the Aβ42 model. N.d.S. wrote the manuscript.

Declaration of Competing Interest

The authors declare that they have no competing interests.

Acknowledgments

We are grateful to Susan Lindquist for providing the yeast strains and plasmids and to Sebastian Treusch for insightful discussions. This work was supported by an EU FP7-ERC starting grant (FP7-ERC-StG-337965), “Foerderungsprofessur” and Sinergia grants from the Swiss National Science Foundation (SNSF) (grants PP00P3_133670 and SNF CRSII5_177195) and a Personalized Health and Related Technologies (PHRT) grant (PHRT-506). P.P. also acknowledges funding from the Gelu Foundation. V.C. was supported by an EMBO short-term postdoctoral fellowship (ASTF 541-2015). Ilaria Piazza was supported by an EMBO long-term postdoctoral fellowship (ALTF 846-2014).

References

[1] T.Q. Melo, S.J.C.V.M. Copray, M.F.R. Ferrari, Alpha-synuclein toxicity on protein quality control, mitochondria and endoplasmic reticulum, Neurochem. Res. 43 (2018) 2212–2223, https://doi.org/10.1007/s11064-018-2673-x.
[2] H. Yang, H.-Y. Hu, Sequestration of cellular interacting partners by protein aggregates: implication in a loss-of-function pathology, FEBS J. 283 (2016) 3705–3717, https://doi.org/10.1111/febs.13722.
[3] C. Hetz, S. Saxena, ER stress and the unfolded protein response in neurodegeneration, Nat. Rev. Neurol. 13 (2017) 477–491, https://doi.org/10.1038/nrneurol.2017.99.
[4] D. Mookherjee, P. Majumder, R. Mukherjee, D. Chatterjee, Z. Kaul, S. Das, R. Sougrat, S. Chakrabarti, O. Chakrabarti, Cytosolic aggregates in presence of non-translocated proteins perturb endoplasmic reticulum structure and dynamics, Traffic. 20 (2019) 943–960, https://doi.org/10.1111/tra.12694.
[5] M. Stefani, C.M. Dobson, Protein aggregation and aggregate toxicity: new insights into protein folding, misfolding diseases and biological evolution, J. Mol. Med. 81 (2003) 678–699, https://doi.org/10.1007/s00109-003-0464-5.
[6] E.J. Bennett, N.F. Bence, R. Jayakumar, R.R. Kopito, Global impairment of the ubiquitin-proteasome system by nuclear or cytoplasmic protein aggregates precedes inclusion body formation, Mol. Cell 17 (2005) 351–365, https://doi.org/10.1016/j.molcel.2004.12.021.
[7] M. Sunde, L.C. Serpell, M. Bartlam, P.E. Fraser, M.B. Pepys, C.C.F. Blake, Common core structure of amyloid fibrils by synchrotron X-ray diffraction, J. Mol. Biol. 273 (1997) 729–739, https://doi.org/10.1006/jmbi.1997.1348.
[8] R.B. Kantcheva, R. Mason, F. Giorgini, Aggregation-prone proteins modulate Huntingtin inclusion body formation in yeast, PLoS Curr. (2014), https://doi.org/10.1371/currents.hd.501008f3051342c9a5c0cd0f3a5bf3a4.
[9] A. Carija, S. Navarro, N.S. de Groot, S. Ventura, Protein aggregation into insoluble deposits protects from oxidative stress, Redox Biol. 12 (2017) 699–711, https://doi.org/10.1016/j.redox.2017.03.027.
[10] C. Huang, S. Wagner-Valladolid, A.D. Stephens, R. Jung, C. Poudel, T. Sinnige, M.C. Lechler, N. Schörit, M. Lu, R.F. Laine, C.H. Michel, M. Vendruscolo, C.F. Kaminski, G.S.K. Schierle, D.C. David, Intrinsically aggregation-prone proteins form amyloid-like aggregates and contribute to tissue aging in *Caenorhabditis elegans*, Elife 8 (2019), https://doi.org/10.7554/eLife.43059.
[11] A.L. Fink, Protein Aggregation: Folding Aggregates, Inclusion Bodies and Amyloid, http://biomednet.com/elecref/13590278003R0009, (1998).
[12] E. Eenjes, J.M. Dragich, H.H. Kampinga, A. Yamamoto, Distinguishing aggregate formation and aggregate clearance using cell-based assays, J. Cell Sci. 129 (2016) 1260–1270, https://doi.org/10.1242/jcs.179978.
[13] Z.T. Monahan, S.N. Rhoads, D.S. Yee, F.P. Shewmaker, Yeast models of prion-like proteins that cause amyotrophic lateral sclerosis reveal pathogenic mechanisms, Front. Mol. Neurosci. 11 (2018), https://doi.org/10.3389/fnmol.2018.00453.
[14] F.T. Outeiro, S. Lindquist, Yeast cells provide insight into alpha-synuclein biology and pathobiology, Science 302 (2003) 1772–1775, https://doi.org/10.1126/science.1090439.
[15] A.B. Meriin, X. Zhang, X. He, G.P. Newnam, Y.O. Chernoff, M.Y. Sherman, Huntington toxicity in yeast model depends on polyglutamine aggregation mediated by a prion-like protein Rnq1.[Erratum appears in J Cell Biol 2002 Aug 5;158(3):591], J. Cell Biol. 157 (6) (2002) 997–1004.
[16] G.A. Newby, S. Kiriakov, E. Hallacli, C. Kayatekin, P. Tsvetkov, C.P. Mancuso, J.M. Bonner, W.R. Hesse, S. Chakrabortee, A.L. Manogaran, S.W. Liebman, S. Lindquist, A.S. Khalil, A genetic tool to track protein aggregates and control prion inheritance, Cell. 171 (2017) 966–979.e18, https://doi.org/10.1016/j.cell.2017.09.041.
[17] S. Krobitsch, S. Lindquist, Aggregation of Huntingtin in Yeast Varies with the Length of the Polyglutamine Expansion and the Expression of Chaperone Proteins, http://www.pnas.org/content/pnas/97/4/1589.full.pdf, (1999).
[18] H. Voßfeldt, M. Butzlaff, K. Prüßing, R.-A. Ní Chárthaigh, P. Karsten, A. Lankes, S. Hamm, M. Simons, B. Adryan, J.B. Schulz, A. Voigt, Large-scale screen for modifiers of ataxin-3-derived polyglutamine-induced toxicity in Drosophila, PLoS One 7 (2012) e47452, , https://doi.org/10.1371/journal.pone.0047452.
[19] Z. Sun, Z. Diaz, X. Fang, M.P. Hart, A. Chesi, J. Shorter, A.D. Gitler, Molecular determinants and genetic modifiers of aggregation and toxicity for the ALS disease protein FUS/TLS, PLoS Biol. 9 (2011) e1000614, , https://doi.org/10.1371/journal.pbio.1000614.
[20] M. Armakola, M.P. Hart, A.D. Gitler, TDP-43 Toxicity in Yeast, (2011), https://doi.org/10.1016/j.ymeth.2010.11.006.
[21] T.J. Van Ham, R. Breitling, M.A. Swertz, E.A.A. Nollen, Neurodegenerative diseases: lessons from genome-wide screens in small model organisms, EMBO Mol. Med. 1 (2009) 360–370, https://doi.org/10.1002/emmm.200900051.
[22] S. Zhang, R. Binari, R. Zhou, N. Perrimon, A genomewide RNA interference screen for modifiers of aggregates formation by mutant huntingtin in drosophila, Genetics. 184 (2010) 1165–1179, https://doi.org/10.1534/genetics.109.112516.
[23] O. Sin, H. Michels, E.A.A. Nollen, Genetic screens in *Caenorhabditis elegans* models for neurodegenerative diseases, Biochim. Biophys. Acta Mol. basis Dis. 1842 (2014) 1951–1959, https://doi.org/10.1016/j.bbadis.2014.01.015.
[24] S. Treusch, S. Hamamichi, J.L. Goodman, K.E.S. Matlack, C.Y. Chung, V. Baru, J.M. Shulman, A. Parrado, B.J. Bevis, J.S. Valastyan, H. Han, M. Lindhagen-Persson, E.M. Reiman, D.A. Evans, D.A. Bennett, A. Olofsson, P.L. DeJager, R.E. Tanzi, K.A. Caldwell, G.A. Caldwell, S. Lindquist, Functional links between Aβ toxicity, endocytic trafficking, and Alzheimer’s disease risk factors in yeast, Science 334

(2011) 1241–1245, https://doi.org/10.1126/science.1213210.
[25] F. D'Angelo, H. Vignaud, J. Di Martino, B. Salin, A. Devin, C. Cullin, C. Marchal, A yeast model for amyloid- aggregation exemplifies the role of membrane trafficking and PICALM in cytotoxicity, Dis. Model. Mech. (2013), https://doi.org/10.1242/dmm.010108.
[26] S. Nair, M. Traini, I.W. Dawes, G.G. Perrone, Genome-wide Analysis of *Saccharomyces cerevisiae* Identifies Cellular Processes Affecting Intracellular Aggregation of Alzheimer's Amyloid-β42: Importance of Lipid Homeostasis, 25 (2014), https://doi.org/10.1091/mbc.E13-04-0216.
[27] Antony A. Cooper, Aaron D. Gitler, Anil Cashikar, Cole M. Haynes, Kathryn J. Hill, Bhupinder Bhullar, Kangning Liu, Kexiang Xu, Katherine E. Strathearn, Fang Liu, Songsong Cao, Kim A. Caldwell, Guy A. Caldwell, Gerald Marsischky, Richard D. Kolodner, Joshua LaBaer, Jean-Christophe Rochet, Nancy M. Bonini, Susan Lindquist2, a-Synuclein Blocks ER-Golgi Traffic and Rab1 Rescues Neuron Loss in Parkinson's Models, http://science.sciencemag.org/content/sci/313/5785/324.full.pdf, (2006).
[28] S. Ju, D.F. Tardiff, H. Han, K. Divya, Q. Zhong, L.E. Maquat, D.A. Bosco, L.J. Hayward, R.H. Brown, S. Lindquist, D. Ringe, G.A. Petsko, A yeast model of FUS/TLS-dependent cytotoxicity, PLoS Biol. 9 (2011), https://doi.org/10.1371/journal.pbio.1001052.
[29] S.E. Di Gregorio, M.L. Duennwald, ALS yeast models - past success stories and new opportunities, Front Mol Neurosci. 11 (2018 Oct 30) 394.
[30] B.S. Johnson, J.M. McCaffery, S. Lindquist, A.D. Gitler, A yeast TDP-43 proteinopathy model: exploring the molecular determinants of TDP-43 aggregation and cellular toxicity, Proc. Natl. Acad. Sci. U. S. A. 105 (2008) 6439–6444, https://doi.org/10.1073/pnas.0802082105.
[31] M.L. Duennwald, S. Jagadish, P.J. Muchowski, S. Lindquist, Flanking Sequences Profoundly Alter Polyglutamine Toxicity in Yeast, https://www.ncbi.nlm.nih.gov/pmc/articles/PMC1544171/pdf/zpq11045.pdf, (2006).
[32] J. Verghese, J. Abrams, Y. Wang, K.A. Morano, Biology of the heat shock response and protein chaperones: budding yeast (*Saccharomyces cerevisiae*) as a model system, Microbiol. Mol. Biol. Rev. 76 (2012) 115–158, https://doi.org/10.1128/MMBR.05018-11.
[33] E.W.J. Wallace, J.L. Kear-Scott, E.V. Pilipenko, T. Pan, B.A. Budnik, D.A. Drummond Correspondence, M.H. Schwartz, P.R. Laskowski, A.E. Rojek, C.D. Katanski, J.A. Riback, M.F. Dion, A.M. Franks, E.M. Airoldi, D.A. Drummond, Reversible, specific, active aggregates of endogenous proteins assemble upon heat stress article reversible, specific, active aggregates of endogenous proteins assemble upon heat stress, Cell 162 (2015) 1286–1298, https://doi.org/10.1016/j.cell.2015.08.041.
[34] S.J. Humphrey, S. Babak Azimifar, M. Mann, High-throughput Phosphoproteomics Reveals In Vivo Insulin Signaling Dynamics, (2015), https://doi.org/10.1038/nbt.3327.
[35] E.W.J. Wallace, J.L. Kear-Scott, E.V. Pilipenko, M.H. Schwartz, P.R. Laskowski, A.E. Rojek, C.D. Katanski, J.A. Riback, M.F. Dion, A.M. Franks, E.M. Airoldi, T. Pan, B.A. Budnik, D.A. Drummond, Reversible, specific, active aggregates of endogenous proteins assemble upon heat stress HHS Public Access, Cell. 162 (2015) 1286–1298, https://doi.org/10.1016/j.cell.2015.08.041.
[36] M. Ashburner, J.J. Bonner, The induction of gene activity in drosophila by heat shock, Cell. 17 (1979) 241–254, https://doi.org/10.1016/0092-8674(79)90150-8.
[37] K. Richter, M. Haslbeck, J. Buchner, The heat shock response: life on the verge of death, Mol. Cell 40 (2010) 253–266, https://doi.org/10.1016/J.MOLCEL.2010.10.006.
[38] Y. Gong, Y. Kakihara, N. Krogan, J. Greenblatt, A. Emili, Z. Zhang, W.A. Houry, An atlas of chaperone–protein interactions in *Saccharomyces cerevisiae*: implications to protein folding pathways in the cell, Mol. Syst. Biol. 5 (2009), https://doi.org/10.1038/msb.2009.26.
[39] R. Linding, L.J. Jensen, A. Pasculescu, M. Olhovsky, K. Colwill, P. Bork, M.B. Yaffe, T. Pawson, NetworKIN: a resource for exploring cellular phosphorylation networks, Nucleic Acids Res. 36 (2008), https://doi.org/10.1093/nar/gkm902.
[40] D. Berchtold, M. Piccolis, N. Chiaruttini, I. Riezman, H. Riezman, A. Roux, T.C. Walther, R. Loewith, Plasma membrane stress induces relocalization of Slm proteins and activation of TORC2 to promote sphingolipid synthesis, Nat. Cell Biol. 14 (2012) 542–547, https://doi.org/10.1038/ncb2480.
[41] J.C. Schwartz, E.R. Podell, S.S.W. Han, J.D. Berry, K.C. Eggan, T.R. Cech, FUS is sequestered in nuclear aggregates in ALS patient fibroblasts, Mol. Biol. Cell 25 (2014) 2571–2578, https://doi.org/10.1091/mbc.E14-05-1007.
[42] S. Willingham, T.F. Outeiro, M.J. DeVit, S.L. Lindquist, P.J. Muchowski, Yeast genes that enhance the toxicity of a mutant huntingtin fragment or alpha-synuclein, Science 302 (2003) 1769–1772, https://doi.org/10.1126/science.1090389.
[43] E. Yeger-Lotem, L. Riva, L.J. Su, A.D. Gitler, A.G. Cashikar, O.D. King, P.K. Auluck, M.L. Geddie, J.S. Valastyan, D.R. Karger, S. Lindquist, E. Fraenkel, Bridging High-throughput Genetic and Transcriptional Data Reveals Cellular Responses to Alpha-synuclein Toxicity, (2009), https://doi.org/10.1038/ng.337.
[44] H.-J. Kim, A.R. Raphael, E.S. LaDow, L. McGurk, R.A. Weber, J.Q. Trojanowski, V.M.-Y. Lee, S. Finkbeiner, A.D. Gitler, N.M. Bonini, Therapeutic modulation of eIF2α phosphorylation rescues TDP-43 toxicity in amyotrophic lateral sclerosis disease models, Nat. Genet. 46 (2013), https://doi.org/10.1038/ng.2853.
[45] M. Armakola, M.J. Higgins, M.D. Figley, S.J. Barmada, E.A. Scarborough, Z. Diaz, X. Fang, J. Shorter, N.J. Krogan, S. Finkbeiner, R.V. Farese, A.D. Gitler, Inhibition of RNA Lariat Debranching Enzyme Suppresses TDP-43 Toxicity in ALS Disease Models, (2012), https://doi.org/10.1038/ng.2434.
[46] V.N. Uversky, C.J. Oldfield, A.K. Dunker, Intrinsically disordered proteins in human diseases: introducing the D 2 concept, Annu. Rev. Biophys. 37 (2008) 215–246, https://doi.org/10.1146/annurev.biophys.37.032807.125924.
[47] N.P. Reynolds, A. Soragni, M. Rabe, D. Verdes, E. Liverani, S. Handschin, R. Riek, S. Seeger, Mechanism of membrane interaction and disruption by α-synuclein, J. Am. Chem. Soc. 133 (2011) 19366–19375, https://doi.org/10.1021/ja2029848.
[48] A. Moharir, L. Gay, D. Appadurai, J. Keener, M. Babst, Eisosomes are metabolically regulated storage compartments for APC-type nutrient transporters, Mol. Biol. Cell 29 (2018) 2113–2127, https://doi.org/10.1091/mbc.E17-11-0691.
[49] D. Snead, D. Eliezer, Alpha-synuclein function and dysfunction on cellular membranes, Exp. Neurobiol. 23 (2014) 292–313, https://doi.org/10.5607/en.2014.23.4.292.
[50] C.E. Ellis, E.J. Murphy, D.C. Mitchell, M.Y. Golovko, F. Scaglia, G.C. Barceló-Coblijn, R.L. Nussbaum, Mitochondrial lipid abnormality and electron transport chain impairment in mice lacking alpha-synuclein, Mol. Cell. Biol. 25 (2005) 10190–10201, https://doi.org/10.1128/MCB.25.22.10190-10201.2005.
[51] S.M. Heman-Ackah, R. Manzano, J.J.M. Hoozemans, W. Scheper, R. Flynn, W. Haerty, S.A. Cowley, A.R. Bassett, M.J.A. Wood, E. Zürich, Alpha-synuclein induces the unfolded protein response in Parkinson's disease SNCA triplication iPSC-derived neurons, Hum. Mol. Genet. 26 (2017) 4441–4450, https://doi.org/10.1093/hmg/ddx331.
[52] K. Nakamura, V.M. Nemani, F. Azarbal, G. Skibinski, J.M. Levy, K. Egami, L. Munishkina, J. Zhang, B. Gardner, J. Wakabayashi, H. Sesaki, Y. Cheng, S. Finkbeiner, R.L. Nussbaum, E. Masliah, R.H. Edwards, Direct membrane association drives mitochondrial fission by the Parkinson disease-associated protein α-synuclein, J. Biol. Chem. 286 (2011) 20710–20726, https://doi.org/10.1074/jbc.M110.213538.
[53] S. Shavali, H.M. Brown-Borg, M. Ebadi, J. Porter, Mitochondrial localization of alpha-synuclein protein in alpha-synuclein overexpressing cells, Neurosci. Lett. 439 (2008) 125–128, https://doi.org/10.1016/j.neulet.2008.05.005.
[54] L. Devi, V. Raghavendran, B.M. Prabhu, N.G. Avadhani, H.K. Anandatheerthavarada, Mitochondrial import and accumulation of α-synuclein impair complex I in human dopaminergic neuronal cultures and Parkinson disease brain, J. Biol. Chem. 283 (2008) 9089–9100, https://doi.org/10.1074/jbc.M710012200.
[55] V.M. Pozo Devoto, T.L. Falzone, Mitochondrial dynamics in Parkinson's disease: a role for α-synuclein? Dis. Model. Mech. 10 (2017) 1075–1087, https://doi.org/10.1242/dmm.026294.
[56] L. Yang, J. Gal, J. Chen, H. Zhu, Self-assembled FUS Binds Active Chromatin and Regulates Gene Transcription (n.d.), (2020), https://doi.org/10.1073/pnas.1414004111.
[57] S.F. Mitchell, S. Jain, M. She, R. Parker, Global analysis of yeast mRNPs, Nat. Struct. Mol. Biol. 20 (2013) 127–133, https://doi.org/10.1038/nsmb.2468.
[58] M.T. Carrì, N. D'Ambrosi, M. Cozzolino, Pathways to mitochondrial dysfunction in ALS pathogenesis, Biochem. Biophys. Res. Commun. 483 (2017) 1187–1193, https://doi.org/10.1016/J.BBRC.2016.07.055.
[59] K. Mori, N. Ogawa, T. Kawahara, H. Yanagi, T. Yura, mRNA splicing-mediated C-terminal replacement of transcription factor Hac1p is required for efficient activation of the unfolded protein response, Proc. Natl. Acad. Sci. U. S. A. 97 (2000) 4660–4665, https://doi.org/10.1073/pnas.050010197.
[60] S.S. Cao, R.J. Kaufman, Unfolded protein response, Curr. Biol. 22 (2012) R622–R626, https://doi.org/10.1016/J.CUB.2012.07.004.
[61] R.J. Braun, J. Ring, V. Franssens, K. Leuven, B. Bruce Morgan, D. Petranovic, M.M.M. Bisschops, N.R. Agarwal, B. Mmm, X. Chen, B. Ji, K.P. Shanmugavel, Interplay of energetics and ER stress exacerbates Alzheimer's amyloid-β (Aβ) toxicity in yeast, Front. Mol. Neurosci. Artic. Front. Mol. Neurosci. 10 (2017), https://doi.org/10.3389/fnmol.2017.00232 2323389–232.
[62] Q. Shi, G.E. Gibson, Oxidative Stress and Transcriptional Regulation in Alzheimer's Disease (n.d.), (2020), https://doi.org/10.1097/WAD.0b013e31815721c3.
[63] Q. Shi, H. Xu, H. Yu, N. Zhang, Y. Ye, A.G. Estevez, H. Deng, G.E. Gibson, Inactivation and Reactivation of the Mitochondrial α-Ketoglutarate Dehydrogenase Complex, (2011), https://doi.org/10.1074/jbc.M110.203018.
[64] S. Sokolov, A. Pozniakovsky, N. Bocharova, D. Knorre, F. Severin, Expression of an Expanded Polyglutamine Domain in Yeast Causes Death With Apoptotic Markers, (2006), https://doi.org/10.1016/j.bbabio.2006.05.004.
[65] A. Bertolotti, Importance of the subcellular location of protein deposits in neurodegenerative diseases, Curr. Opin. Neurobiol. 51 (2018) 127–133, https://doi.org/10.1016/j.conb.2018.03.004.